crystals

MDPI

Communication

Structural and Luminescent Properties of Heterobimetallic Zinc(II)-Europium(III) Dimer Constructed from N_2O_2-Type Bisoxime and Terephthalic Acid

Wen-Ting Guo, Xiao-Yan Li, Quan-Peng Kang, Jian-Chun Ma and Wen-Kui Dong *

School of Chemical and Biological Engineering, Lanzhou Jiaotong University, Lanzhou 730070, China; gwtzy044@126.com (W.-T.G.); L1401569787@163.com (X.-Y.L.); KQpeng2580@163.com (Q.-P.K.); majc0204@126.com (J.-C.M.)

* Correspondence: dongwk@126.com; Tel.: +86-931-493-8703

Received: 8 March 2018; Accepted: 30 March 2018; Published: 2 April 2018

Abstract: A new heterohexanuclear Zn^{II}–Eu^{III} dimer $[\{(ZnL)_2Eu\}_2(bdc)_2]\cdot 2Cl$ constructed from a N_2O_2-type chelating ligand H_2L (6,6′-Dimethoxy-2,2′-[ethylenedioxybis(nitrilomethylidyne)]diphenol), $Zn(OAc)_2\cdot 2H_2O$, $EuCl_3\cdot 6H_2O$ and H_2bdc (terephthalic acid) was synthesized, and characterized using elemental analyses, IR (Infrared), UV-Vis (Ultraviolet–visible) spectra and X-ray single crystal diffraction method. There are two crystallographically equivalent $[(ZnL)_2Eu]$ moieties in the Zn^{II}–Eu^{III} complex, the two $[(ZnL)_2Eu]$ moieties are linked by two bdc^{2-} ligand leading to a heterohexanuclear dimer, in which the carboxylato groups bridge the Zn^{II} and Eu^{III} atoms. Furthermore, the luminescence properties of H_2L and its Zn^{II}–Eu^{III} complex have been studied.

Keywords: N_2O_2-type bisoxime; terephthalic acid; heterobimetallic complex; crystal structure; luminescence property

1. Introduction

Salen-type N_2O_2 ligands are easily obtained via the reaction of salicylaldehyde or its derivatives with diamines, can coordinated to transition metal ions in a N_2O_2 tetradentate chelating mode to form stable mono- or multinuclear complexes [1–6]. Salen- and salamo-type complexes have been extensively investigated in organometallic chemistry and modern coordination chemistry for several decades [7–11], their complexes are well-known for their potential applications in many areas, such as catalysts [12,13], biological fields [14–21], supramolecular buildings [22–26], molecular recognitions [27–31], magnetic [32–37] and luminescence [38–45] materials and so forth. Self-assembling processes of a metallohost complex with auxiliary organic ligands are usually utilized in the building of metal-organic framework (MOF) materials [46,47]. When 3-alkoxy groups are introduced of salicylidene moieties, an O_4 coordination site composed of the alkoxy and phenoxo oxygen atoms are produced in addition to the N_2O_2 site [48–51]. The O_4 site of 3-alkoxy-induced Salen-type ligand is suitable for lanthanide(III) atoms to prepare 3d–4f heteronuclear complexes. These 3d–4f heterobimetallic Salen-type complexes have been diffusely studied [14,34,37,44] in which acetate (OAc^-) combine plays a key role in assembling 3d and 4f metals [52], however, 3d–4f heterobimetallic Salamo-type complexes have been rarely reported, especially the auxiliary ligands were introduced [53].

Herein, a newly 3d–4f heterobimetallic dimer, $[\{(ZnL)_2Eu\}_2(bdc)_2]\cdot 2Cl$ has been obtained by a N_2O_2-type chelating ligand H_2L and auxiliary ligand bdc^{2-}. In addition, the luminescence properties of H_2L and its Zn^{II}–Eu^{III} complex have been studied.

2. Experimental Section

2.1. Materials and Measurements

2-Hydroxy-3-methoxybenzaldehyde (99%) was purchased from Alfa Aesar (New York, NY, USA), while Tianjin Chemical Reagent Factory (Tianjin, China) supplied the remaining reagents. Elemental analyses for zinc and europium were detected by IRIS ER/S-WP-1 ICP atomic emission spectrometer (Elementar, Berlin, Germany), elemental analyses for Carbon, hydrogen and nitrogen were analyzed using GmbH VariuoEL V3.00 automatic elemental analysis instrument (Elementar, Berlin, Germany). IR spectra (4000–400 cm^{-1}) were recorded on a Vertex 70 FT-IR (Fourier Transform infrared) spectrophotometer (Bruker, Billerica, MA, USA), with samples prepared as KBr pellets. UV-vis absorption spectra were measured on a Shimadzu UV-3900 spectrometer (Shimadzu, Tokyo, Japan). ^{1}H NMR (Nuclear Magnetic Resonance) spectra were determined by German Bruker AVANCE DRX-400/600 spectroscopy (Bruker AVANCE, Billerica, MA, USA). Fluorescence spectra were recorded on a F-7000 FL spectrophotometer (Hitachi, Tokyo, Japan). X-ray single-crystal structure was determined on a SuperNova Dual (Cu at zero) four-circle diffractometer.

2.2. Synthesis of H_2L

The ligand 6,6′-dimethoxy-2,2′-[ethylenedioxybis(nitrilomethylidyne)]diphenol (H_2L) was synthesized in accordance with the earlier reported method [54]. Yield: 83.6%. m.p: 131–132 °C. ^{1}H NMR (400 MHz, $CDCl_3$), δ 3.91 (s, 6H), 4.49 (s, 4H), 6.83 (dd, J = 7.9, 1.9 Hz, 2H), 6.86 (t, J = 7.9 Hz, 2H), 6.91 (dd, J = 7.9, 1.9 Hz, 2H), 8.26 (s, 2H), 9.74 (s, 2H). IR (KBr, cm^{-1}): 3131 [ν(O–H)], 1618 [ν(C=N)], 1253 [ν(Ar-O)]. UV-Vis (CH_3OH), λ_{max} (nm) (ε_{max}): 224, 270 and 318 nm (3.0×10^{-5} M). Anal. Calcd for $C_{18}H_{20}N_2O_6$ (%): C 59.99; H 5.59; N 7.77. Found: C 60.29; H 5.42; N 7.56.

2.3. Synthesis of the Zn^{II}–Eu^{III} Complex

To a solution of H_2L (7.20 mg, 0.02 mmol) in $CHCl_3$ (3 mL) was added $Zn(OAc)_2\cdot 2H_2O$ (4.39 mg, 0.02 mmol) and $EuCl_3\cdot 6H_2O$ (7.33 mg, 0.02 mmol) in CH_3CH_2OH (2 mL). After the mixture was stirred for about 15 min at r.t., a solution of H_2bdc (3.32 mg, 0.02 mmol) in DMF (1 mL) was added dropwise and continued to stir for 15 min. The mixture was filtered, and the filtrate was obtained. Several yellow block single crystals were obtained via slow evaporation of the mixture solution in open atmosphere for almost two weeks. (Scheme 1) Yield: 72.6%. IR (KBr, cm^{-1}): 1607 [ν(C=N)], 1217 [ν(Ar–O)]. UV-Vis (CH_3OH), λ_{max} (nm) (ε_{max}): 233, 279 and 352 nm (3.0×10^{-5} M). Anal. Calcd for $C_{88}H_{80}Cl_2Eu_2Zn_4N_8O_{32}$ (%): C, 44.08; H, 3.36; N, 4.67; Zn, 10.91; Eu, 12.67. Found: C, 44.29; H, 4.45; N, 4.51; Zn, 11.02; Eu, 12.43.

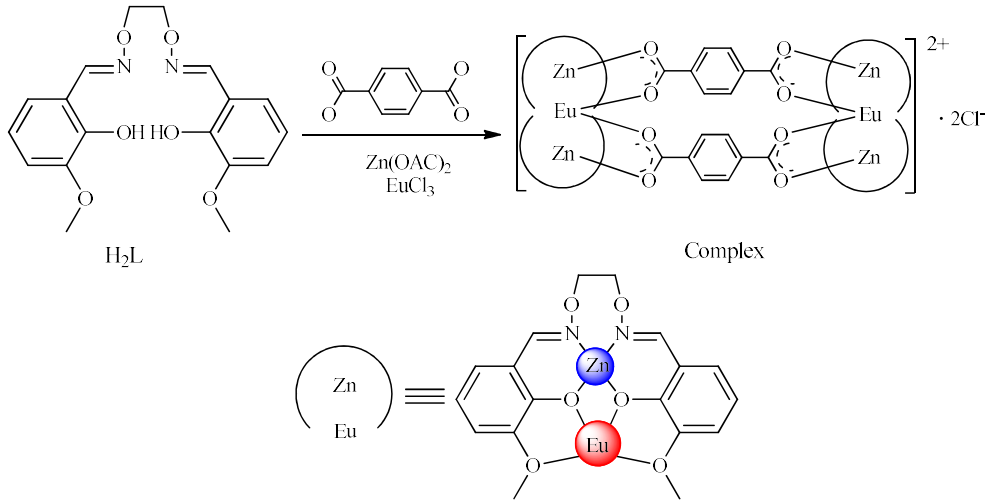

Scheme 1. Synthesis of the Zn^{II}–Eu^{III} complex.

2.4. X-ray Crystal Structure Determinations for the Zn^{II}–Eu^{III} Complex

The single crystal diffractometer provides a monochromatic beam of Mo-Kα radiation (0.71073 Å) produced from a sealed Mo X-ray tube using Graphite monochromator and was used for obtaining crystal data for the Zn^{II}–Eu^{III} complex at 291(2) K, respectively. The LP factor and semi-empirical absorption were using SADABS. The structures of the Zn^{II}–Eu^{III} complex were solved via the direct methods (SHELXS-2016) [55], and all hydrogen atoms were included at the calculated positions and constrained to ride on their parent atoms. All non-hydrogen atoms were refined anisotropically using a full-matrix least-squares procedure on F^2 with SHELXL-2016 [56]. In the X-ray structure refinement, however, the solvent molecules of the complex could not be located because of its high thermal disorder, and the final structure model was refined without the solvent molecules by using a SQUEEZE routine of PLATON. Table 1 shows the data collection and refinements of the Zn^{II}–Eu^{III} complex. Supplementary crystallographic data for this paper have been deposited at Cambridge Crystallographic Data Centre (1,828,198) and can be obtained free of charge via www.ccdc.cam.ac.uk/conts/retrieving.html.

Table 1. Crystal data and refinement parameters for the Zn^{II}–Eu^{III} complex.

	Zn^{II}–Eu^{III} Complex
Formula	$C_{88}H_{80}Cl_2Eu_2Zn_4N_8O_{32}$
Formula weight	2397.90
Temperature (K)	291(2)
Wavelength (Å)	0.71073
Crystal system	triclinic
Space group	*P*-1
a (Å)	12.5053(15)
b (Å)	16.125(3)
c (Å)	16.5068(13)
α (°)	68.518(13)
β (°)	82.216(12)
γ (°)	86.716(14)
V (Å^3)	3068.6(8)
Z	1
D_{calc} (g·cm^{-3})	1.298
μ (mm^{-1})	1.885
F (000)	1200
Crystal size (mm)	0.18 × 0.20 × 0.22
θ Range (°)	2.123–25.682

Table 1. *Cont.*

	Zn^{II}–Eu^{III} Complex
Index ranges	$-14 \leq h \leq 15$ $-18 \leq k \leq 19$ $0 \leq l \leq 20$
Reflections collected	11,612
Independent reflections	11,611
R_{int}	0.0726
Completeness to θ	99.6% (θ = 25.242)
Data/restraints/parameters	11611/0/627
GOF	1.029
Final R_1, wR_2 indices	0.0482, 0.1182
R_1, wR_2 indices (all data)	0.0644, 0.1215
Largest differences peak and hole (e Å^{-3})	1.696/−0.554

GOF: Goodness-of-fit on F.

3. Results and Discussion

3.1. IR Spectra

The IR spectra of H_2L and its corresponding Zn^{II}–Eu^{III} complex exhibited different bands in the region of 4000–400 cm^{-1} region (Table 2). It is obvious that the ν(O–H) absorption band was near 3131 cm^{-1} in the spectrum of H_2L. The free ligand exhibited a characteristic C=N stretching band at 1618 cm^{-1}, while the Zn^{II}–Eu^{III} complex appeared at 1607 cm^{-1}. The characteristic C=N stretching frequency is shifted to lower frequency, which indicating that the metal(II) atoms are bonded by oxime N atoms [57]. The Ar–O stretching frequencies appeared as a strong band within 1265–1213 cm^{-1} range as reported for similar Salen-type ligands [58]. Meanwhile, the free ligand H_2L exhibited an Ar–O stretching frequency at 1253 cm^{-1}, while the Zn^{II}–Eu^{III} complex appeared at 1217 cm^{-1}, the Ar–O stretching frequency is shifted to lower frequency, indicating that the M–O bonds are formed [59]. In addition, characteristic absorption bands of the carboxylato ions are observed, the absorption bands $\nu_{as}(COO^-)$ and $\nu_s(COO^-)$ of the Zn^{II}–Eu^{III} complex are 1572 and 1468 cm^{-1}, respectively, indicating the bidentate coordination mode of carboxylato ions [60], which is in consistent with the X-ray diffraction result obtained for the Zn^{II}–Eu^{III} complex.

Table 2. The major IR spectra of H_2L and its Zn^{II}–Eu^{III} complex (cm^{-1}).

Compound	$\nu_{(O–H)}$	$\nu_{(C=N)}$	$\nu_{(Ar–O)}$	$\nu_{(C=C)}$	$\nu_{s(COO^-)}$	$\nu_{as(COO^-)}$
H_2L	3131	1618	1253	1374		
Complex	-	1607	1217	1314	1468	1572

3.2. UV–Vis Spectra

UV–Vis absorption spectra of H_2L and its corresponding Zn^{II}–Eu^{III} complex were determined in 3.0×10^{-5} M methanol solution, as depicted in Figure 1. The absorption spectrum of the Zn^{II}–Eu^{III} complex is different from that of H_2L. UV–Vis spectrum of H_2L exhibited three absorptions at ca. 224, 270 and 318 nm. The absorptions at 224 and 270 nm can be assigned to π–π^* transitions of the benzene rings, while the absorption at 318 nm can be attributed to π–π^* transition of C=N groups [61]. Compared with the absorption peak of H_2L, the corresponding absorption peaks at ca. 233 and 279 nm are observed in the Zn^{II}–Eu^{III} complex, which were bathochromically shifted, indicating the coordination of metal atoms with the ligand [62]. Meanwhile, a new absorption peak was observed at ca. 352 nm in the Zn^{II}–Eu^{III} complex, and assigned to L→M charge-transfer (LMCT) transitions, which is characteristic of the transition metal complexes with Salen-type N_2O_2 coordination spheres [63].

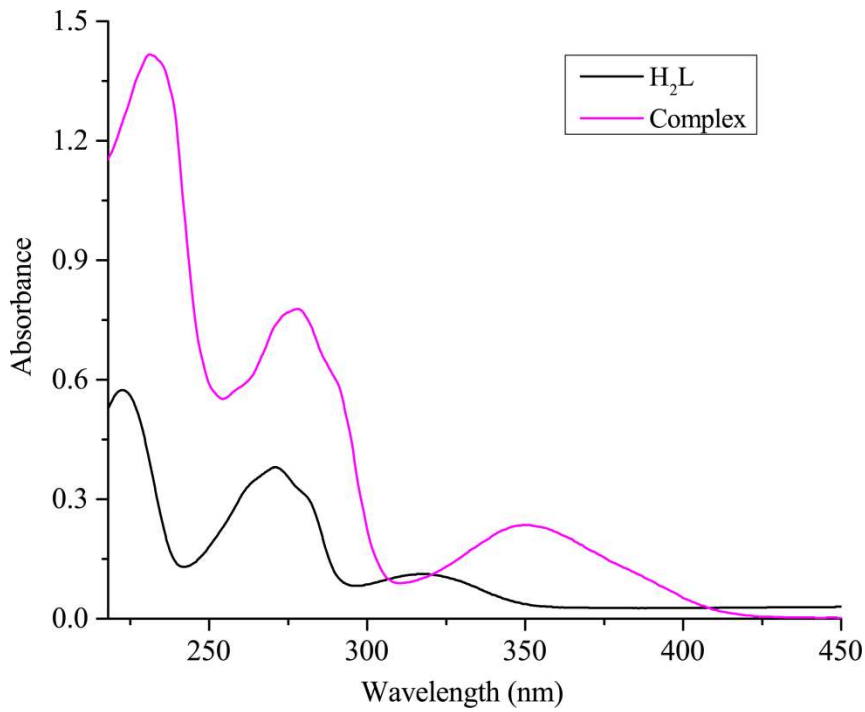

Figure 1. The UV–Vis spectra of H_2L and its Zn^{II}–Eu^{III} complex (cm^{-1}).

3.3. Description of the Crystal Structure

The crystal structure of the heterohexanuclear Zn^{II}–Eu^{III} complex is depicted in Figure 2 and Table 3, the crystallographic data revealed that the Zn^{II}–Eu^{III} complex crystallizes in the triclinic space group *P*-1 with Z = 1. By the reaction of H_2L with $Zn(OAc)_2{\cdot}2H_2O$, $EuCl_3{\cdot}6H_2O$ and H_2bdc, a heterohexanuclear Zn^{II}–Eu^{III} complex is formed: $[\{(ZnL)_2Eu\}_2(bdc)_2]{\cdot}2Cl$, the molecular structure of the Zn^{II}–Eu^{III} complex composes of four Zn^{II} atoms, two Eu^{III} atoms, four deprotonated $(L)^{2-}$ ligands, two auxiliary ligand bdc^{2-} moieties. Each Zn^{II} atom (Zn1 or Zn2) is located at the N_2O_2 coordination spheres of Salamo moieties, they are penta-coordinated by two oxime nitrogen (N1, N2 or N3, N4) atoms, two deprotonated phenoxo-oxygen (O2, O5 or O8, O11) atoms of the $(L)^{2-}$ units and one oxygen (O16 or O13) atom comes from the coordinated terephthalic acid molecule. The coordination environment around all the Zn^{II} atoms are best described as slightly distorted triangular bipyramid geometries [64], which were deduced by calculating the values of τ_1 = 0.539 and τ_2 = 0.6125 [65], respectively. The equatorial coordination sites with the distances of N2–Zn1 = 2.046(5) Å, O2–Zn1 = 2.000(4) Å and O16–Zn1 = 1.983(4) Å, and the axial position with the distances of O5–Zn1 = 2.052(4) and N1–Zn1 = 2.116(5) Å (Table 3). The dihedral angle between coordination planes of N1–Zn1–O2 and N2–Zn1–O5 is 51.84(5)°. The dihedral angle between coordination planes of N1–Zn2–O2 and N2–Zn2–O5 is 55.37(2)°.

In addition, the central Eu^{III} atom is located in a deca-coordinated O_{10} environment, the coordination sphere of the central Eu^{III} atom contains eight oxygen atoms (O1, O2, O5, O6 and O7, O8, O11, O12) from two deprotonated $(L)^{2-}$ units and two oxygen atoms (O14 and O15) comes from the coordinated bdc^{2-} ions. Thus, the deca-coordinated Eu^{III} atom adopts a distorted bicapped square antiprism coordination arrangement. The primary Eu–O distances are in the normal ranges of 2.378(4)–2.844(4) Å (Table 3). The dihedral angle between the O2–Zn1–O5 and O2–Eu1–O5 planes is 32.41(4)°.

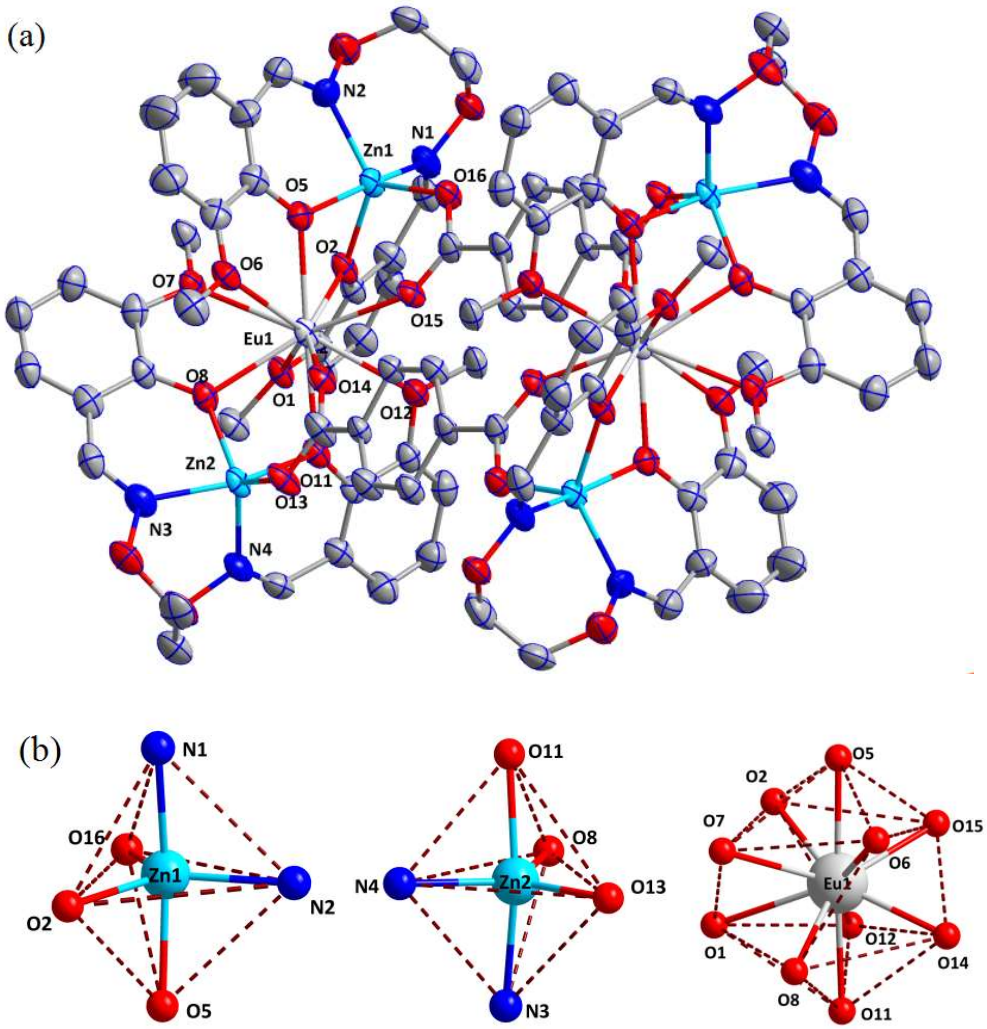

Figure 2. (**a**) Molecular structure and atom numberings of the Zn^{II}–Eu^{III} complex with 30% probability displacement ellipsoids (hydrogen atoms are omitted for clarity); (**b**) coordination polyhedrons for Zn^{II} and Eu^{III} atoms.

Table 3. Selected bond lengths (Å) and angles (°) of the Zn^{II}–Eu^{III} complex.

Bond	Lengths	Bond	Lengths
N1–Zn1	2.116(5)	N2–Zn1	2.046(5)
O2–Zn1	2.000(4)	O5–Zn1	2.052(4)
O16–Zn1	1.983(4)	N3–Zn2	2.135(5)
N4–Zn2	2.005(5)	O8–Zn2	1.965(4)
O11–Zn2	2.056(3)	O13–Zn2	1.986(3)
Eu1–O5	2.383(4)	Eu1–O2	2.385(3)
Eu1–O15	2.418(3)	Eu1–O8	2.445(4)
Eu1–O11	2.452(4)	Eu1–O1	2.637(3)
Eu1–O7	2.670(4)	Eu1–O12	2.832(4)
Eu1–O6	2.844(4)	Eu1–O14	2.378(4)
Bond	**Angles**	**Bond**	**Angles**
O16–Zn1–O2	111.62(15)	O16–Zn1–O5	97.39(15)
O2–Zn1–O5	76.97(14)	O16–Zn1–N2	118.07(18)
O2–Zn1–N2	129.54(18)	O5–Zn1–N2	88.3(2)
O16–Zn1–N1	97.88(17)	O2–Zn1–N1	88.36(17)
O5–Zn1–N1	161.88(16)	N2–Zn1–N1	93.1(2)
O8–Zn2–O13	114.67(16)	O8–Zn2–N4	125.97(18)

Table 3. *Cont.*

Bond	Angles	Bond	Angles
O13–Zn2–N4	118.96(19)	O8–Zn2–O11	79.89(15)
O13–Zn2–O11	97.49(15)	N4–Zn2–O11	87.20(18)
O8–Zn2–N3	86.80(19)	O13–Zn2–N3	98.07(17)
N4–Zn2–N3	91.8(2)	O11–Zn2–N3	162.72(17)
O14–Eu1–O5	107.44(12)	O14–Eu1–O2	151.04(12)
O5–Eu1–O2	63.88(13)	O14–Eu1–O15	72.43(11)
O5–Eu1–O15	71.56(12)	O2–Eu1–O15	78.67(12)
O14–Eu1–O8	77.38(12)	O5–Eu1–O8	117.81(13)
O2–Eu1–O8	131.54(12)	O15–Eu1–O8	149.80(12)
O14–Eu1–O11	70.71(11)	O5–Eu1–O11	177.52(11)
O2–Eu1–O11	116.88(12)	O15–Eu1–O11	106.14(12)
O8–Eu1–O11	63.68(13)	O14–Eu1–O1	138.67(11)
O5–Eu1–O1	113.38(12)	O2–Eu1–O1	60.79(11)
O15–Eu1–O1	126.52(11)	O8–Eu1–O1	78.26(11)
O11–Eu1–O1	68.66(11)	O14–Eu1–O7	125.52(12)
O5–Eu1–O7	69.27(12)	O2–Eu1–O7	79.07(12)
O15–Eu1–O7	140.37(12)	O8–Eu1–O7	60.58(12)
O11–Eu1–O7	113.11(12)	O1–Eu1–O7	66.58(12)
O14–Eu1–O12	97.83(12)	O5–Eu1–O12	121.21(12)
O2–Eu1–O12	68.48(12)	O15–Eu1–O12	67.04(12)
O8–Eu1–O12	119.14(12)	O11–Eu1–O12	57.94(11)
O1–Eu1–O12	66.45(11)	O7–Eu1–O12	131.59(12)
O14–Eu1–O6	65.87(13)	O5–Eu1–O6	59.08(12)
O2–Eu1–O6	120.77(13)	O15–Eu1–O6	97.08(12)
O8–Eu1–O6	69.06(12)	O11–Eu1–O6	120.81(12)
O1–Eu1–O6	132.51(11)	O7–Eu1–O6	67.58(12)
O12–Eu1–O6	160.75(11)		

As depicted in Figure 3 and Table 4, In the crystal structure of the Zn^{II}–Eu^{III} complex, five pairs of intramolecular C1–H1B···O8, C9–H9A···O16, C19–H19B···O2, C36–H36B···O15 and C43–H43···O13 interactions are formed [66–68], which plays a vital role in constructing and stabilizing the complex molecule. The donors (C1–H1B and C19–H19B) from 3-methoxy of the $(L)^{2-}$ units form hydrogen bonding with oxygen atoms (O8 and O2) of phenoxo-oxygen of the $(L)^{2-}$ units as hydrogen bonding receptors. The donors (C9–H9A and C36–H36B) from the $(L)^{2-}$ units form hydrogen bonding with oxygen atom (O16 and O15) of the bdc^{2-} moiety as hydrogen bonding receptor. The donor (C43–H43) from bdc^{2-} moiety formed hydrogen bonding with oxygen atom (O13) of bdc^{2-} moiety as hydrogen bonding receptor.

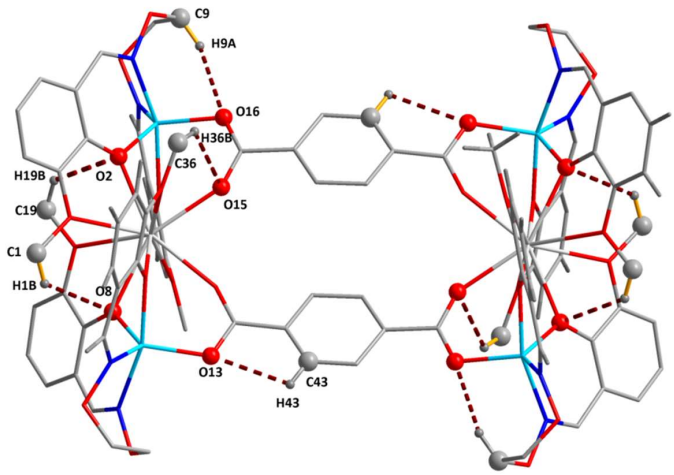

Figure 3. View of the intramolecular hydrogen bondings of the Zn^{II}–Eu^{III} complex.

Table 4. Hydrogen bonding interactions (Å, °) of the Zn^{II}–Eu^{III} complex.

D–H···A	D–H	H···A	D···A	D–H···A
C1–H1B···O8	0.96	2.56	3.281(6)	132
C9–H9A···O16	0.97	2.41	3.311(10)	154
C19–H19B···O2	0.96	2.55	3.280(8)	133
C36–H36B···O15	0.96	2.54	3.148(7)	122
C43–H43···O13	0.93	2.46	2.773(7)	100

3.4. Luminescence Spectra

The luminescence spectra of H_2L and its Zn^{II}–Eu^{III} complex were measured in 3.0×10^{-5} M methanol solution (Figure 4). The ligand H_2L exhibited an intense emission peak at ca. 442 nm upon excitation at 352 nm which should be assigned to intra-ligand π–π* transition [69,70]. The Zn^{II}–Eu^{III} complex showed slightly weak photoluminescence with maximum emission at ca. 445 nm upon excitation at 352 nm. In the luminescence spectra, only a band at ca. 375–650 nm instead of the f–f emission expected for Eu^{III} ions [71]. In the Zn^{II}–Eu^{III} complex, the emission from Eu^{III} is quenched which may due to thermal quenching of the $^5D_0$ level of Eu^{III} by LMCT process [72]. The concentration of H_2L and its Zn^{II}–Eu^{III} complex used are all 3.0×10^{-5} M, indicating that the relative strengths of H_2L and its Zn^{II}–Eu^{III} complex are independent of the concentration.

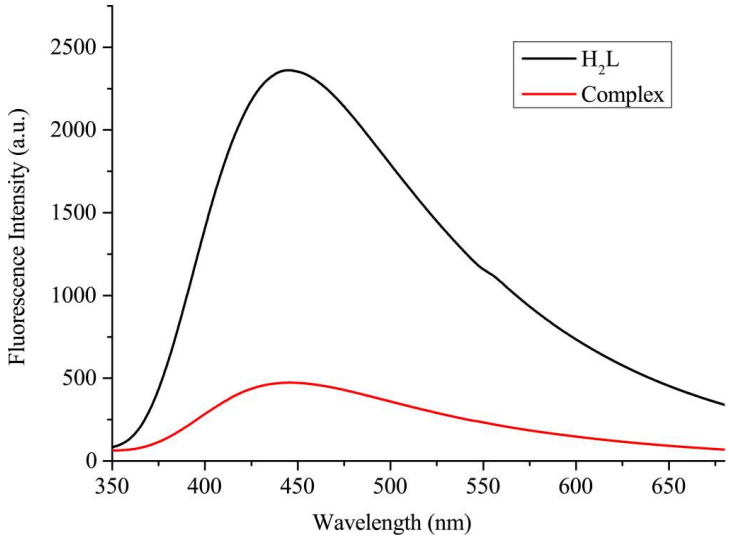

Figure 4. Luminescence spectra of H_2L and its Zn^{II}–Eu^{III} complex in methanol (3.0×10^{-5} M) upon excitation at 352 nm.

4. Conclusions

In summary, a new heterohexanuclear Zn^{II}–Eu^{III} dimer was synthesized and characterized. In the Zn^{II}–Eu^{III} complex, there are two crystallographically equivalent $[(ZnL)_2Eu]$ moieties which are linked by two bdc^{2-} auxiliary ligand leading to a heterohexanuclear dimer. The Zn^{II} atom possesses a penta-coordinated environment and adopts a slightly distorted triangular bipyramid geometry and the deca-coordinated Eu^{III} atom adopts a distorted bicapped square antiprism. In addition, the luminescence spectrum of the Zn^{II}–Eu^{III} complex indicated that the coordination of Eu^{III} atoms led to the fluorescence quenching of H_2L.

Acknowledgments: This work was supported by the National Natural Science Foundation of China (21761018) and the Program for Excellent Team of Scientific Research in Lanzhou Jiaotong University (201706), which is gratefully acknowledged.

Author Contributions: Wen-Kui Dong conceived and designed the experiments; Quan-Peng Kang and Xiao-Yan Li performed the experiments; Jian-Chun Ma analyzed the data; Wen-Ting Guo contributed reagents/materials/analysis tools; Xiao-Yan Li and Wen-Ting Guo wrote the paper.

Conflicts of Interest: The authors declare no competing financial interests.

References

1. Dong, X.Y.; Akogun, S.F.; Zhou, W.M.; Dong, W.K. Tetranuclear Zn(II) complex based on an asymmetrical salamo-type chelating ligand: Synthesis, structural characterization, and fluorescence property. *J. Chin. Chem. Soc.* **2017**, *64*, 412–419. [CrossRef]
2. Wu, H.L.; Bai, Y.C.; Zhang, Y.H.; Li, Z.; Wu, M.C.; Chen, C.Y.; Zhang, J.W. Synthesis, crystal structure, antioxidation and DNA-binding properties of a dinuclear copper(II) complex with bis(*N*-salicylidene)-3-oxapentane-1,5-diamine. *J. Coord. Chem.* **2014**, *67*, 3054–3066. [CrossRef]
3. Chen, C.Y.; Zhang, J.W.; Zhang, Y.H.; Yang, Z.H.; Wu, H.L. Gadolinium(III) and dysprosium(III) complexes with a Schiff base bis(*N*-salicylidene)-3-oxapentane-1,5-diamine: Synthesis, characterization, antioxidation, and DNA-binding studies. *J. Coord. Chem.* **2015**, *68*, 1054–1071. [CrossRef]
4. Sun, Y.X.; Zhang, Y.J.; Meng, W.S.; Li, X.R.; Lu, R.E. Synthesis and crystal structure of new nickel(II) complex with Salen-type bisoxime ligand. *Asian J. Chem.* **2014**, *26*, 416–418.
5. Chai, L.Q.; Huang, J.J.; Zhang, H.S.; Zhang, Y.L.; Zhang, J.Y.; Li, Y.X. An unexpected cobalt(III) complex containing a Schiff base ligand: Synthesis, crystal structure, spectroscopic behavior, electrochemical property and SOD-like activity. *Spectrochim. Acta A* **2014**, *131*, 526–533. [CrossRef] [PubMed]
6. Sun, Y.X.; Gao, X.H. Synthesis, characterization, and crystal structure of a new Cu^{II} complex with salen-type ligand. *Synth. React. Inorg. Met.-Org. Nano-Met. Chem.* **2011**, *41*, 973–978. [CrossRef]
7. Wang, P.; Zhao, L. Synthesis, structure and spectroscopic properties of the trinuclear cobalt(II) and nickel(II) complexes based on 2-hydroxynaphthaldehyde and bis(aminooxy)alkane. *Spectrochim. Acta Part A* **2015**, *135*, 342–350. [CrossRef] [PubMed]
8. Dong, X.Y.; Sun, Y.X.; Wang, L.; Li, L. Synthesis and structure of a penta- and hexa-coordinated tri-nuclear cobalt(II) complex. *J. Chem. Res.* **2012**, *36*, 387–390. [CrossRef]
9. Wang, P.; Zhao, L. An infinite 2D supramolecular cobalt(II) complex based on an asymmetric Salamo-type ligand: Synthesis, crystal structure, and spectral properties. *Synth. React. Inorg. Met.-Org. Nano-Met. Chem.* **2016**, *46*, 1095–1101. [CrossRef]
10. Sun, Y.X.; Xu, L.; Zhao, T.H.; Liu, S.H.; Liu, G.H.; Dong, X.T. Synthesis and crystal structure of a 3D supramolecular copper(II) complex with 1-(3-{[(E)-3-bromo-5-chloro-2-hydroxybenzylidene]amino}phenyl) ethanone oxime. *Synth. React. Inorg. Met.-Org. Nano-Met. Chem.* **2013**, *43*, 509–513. [CrossRef]
11. Zhang, H.; Dong, W.K.; Zhang, Y.; Akogun, S.F. Naphthalenediol-based bis(Salamo)-type homo- and heterotrinuclear cobalt(II) complexes: Syntheses, structures and magnetic properties. *Polyhedron* **2017**, *133*, 279–293. [CrossRef]
12. Li, X.Y.; Chen, L.; Gao, L.; Zhang, Y.; Akogun, S.F.; Dong, W.K. Syntheses, crystal structures and catalytic activities of two solvent-induced homotrinuclear Co(II) complexes with a naphthalenediol-based bis(Salamo)-type tetraoxime ligand. *RSC Adv.* **2017**, *7*, 35905–35916. [CrossRef]
13. Li, L.H.; Dong, W.K.; Zhang, Y.; Akogun, S.F.; Xu, L. Syntheses, structures and catecholase activities of homo-and hetero-trinuclear cobalt(II) complexes constructed from an acyclic naphthalenediol-based bis(salamo)-type ligand. *Appl. Organomet. Chem.* **2017**, *31*, e3818. [CrossRef]
14. Wu, H.L.; Bai, Y.C.; Zhang, Y.H.; Pan, G.L.; Kong, J.; Shi, F.; Wang, X.L. Two lanthanide(III) complexes based on the schiff base *N*,*N*-Bis(salicylidene)-1,5-diamino-3-oxapentane: Synthesis, characterization, DNA-binding properties, and antioxidation. *Z. Anorg. Allg. Chem.* **2014**, *640*, 2062–2071. [CrossRef]
15. Wu, H.L.; Bai, Y.; Yuan, J.K.; Wang, H.; Pan, G.L.; Fan, X.Y.; Kong, J. A zinc(II) complex with tris(2-(*N*-methyl)benzimidazlylmethyl)amine and salicylate: Synthesis, crystal structure, and DNA-binding. *J. Coord. Chem.* **2012**, *65*, 2839–2851. [CrossRef]
16. Wu, H.L.; Pan, G.L.; Wang, H.; Wang, X.L.; Bai, Y.C.; Zhang, Y.H. Study on synthesis, crystal structure, antioxidant and DNA-binding of mono-, di- and poly-nuclear lanthanides complexes with bis(*N*-salicylidene)-3-oxapentane-1,5-diamine. *J. Photochem. Photobiol. B Biol.* **2014**, *135*, 33–43. [CrossRef] [PubMed]

17. Wu, H.L.; Wang, C.P.; Wang, F.; Peng, H.P.; Zhang, H.; Bai, Y.C. A new manganese(III) complex from bis(5-methylsalicylaldehyde)-3-oxapentane-1,5-diamine: Synthesis, characterization, antioxidant activity and luminescence. *J. Chin. Chem. Soc.* **2015**, *62*, 1028–1034. [CrossRef]
18. Wu, H.L.; Pan, G.L.; Bai, Y.C.; Wang, H.; Kong, J.; Shi, F.R.; Zhang, Y.H.; Wang, X.L. A Schiff base bis(*N*-salicylidene)-3-oxapentane-1,5-diamine and its yttrium(III) complex: Synthesis, crystal structure, DNA-binding properties, and antioxidant activities. *J. Coord. Chem.* **2013**, *66*, 2634–2646. [CrossRef]
19. Li, X.Y.; Kang, Q.P.; Liu, L.Z.; Ma, J.C.; Dong, W.K. Trinuclear Co(II) and Mononuclear Ni(II) Salamo-Type Bisoxime Coordination Compounds. *Crystals* **2018**, *8*, 43. [CrossRef]
20. Wu, H.L.; Pan, G.L.; Bai, Y.C.; Wang, H.; Kong, J. Synthesis, structure, antioxidation, and DNA-bindingstudies of a binuclear ytterbium(III) complex with bis(*N*-salicylidene)-3-oxapentane-1,5-diamine. *Res. Chem. Intermed.* **2015**, *41*, 3375–3388. [CrossRef]
21. Wu, H.L.; Pan, G.L.; Bai, Y.C.; Wang, H.; Kong, J.; Shi, F.; Zhang, Y.H.; Wang, X.L. Preparation, structure, DNA-binding properties, and antioxidant activities of a homodinuclear erbium(III) complex with a pentadentate Schiff base ligand. *J. Chem. Res.* **2014**, *38*, 211–217. [CrossRef]
22. Sun, Y.X.; Zhang, S.T.; Ren, Z.L.; Dong, X.Y.; Wang, L. Synthesis, characterization, and crystal structure of a new supramolecular Cd^{II} complex with halogen-substituted salen-type bisoxime. *Synth. React. Inorg. Met.-Org. Nano-Met. Chem.* **2013**, *43*, 995–1000. [CrossRef]
23. Sun, Y.X.; Wang, L.; Dong, X.Y.; Ren, Z.L.; Meng, W.S. Synthesis, characterization, and crystal structure of a supramolecular Co^{II} complex containing Salen-type bisoxime. *Synth. React. Inorg. Met.-Org. Nano-Met. Chem.* **2013**, *43*, 599–603. [CrossRef]
24. Dong, W.K.; Wang, Z.K.; Li, G.; Zhao, M.M.; Dong, X.Y.; Liu, S.H. Syntheses, crystal structures, and properties of a Salamo-type tetradentate chelating ligand and its pentacoordinated copper(II) complex. *Z. Anorg. Allg. Chem.* **2013**, *639*, 2263–2268. [CrossRef]
25. Chai, L.Q.; Zhang, K.Y.; Tang, L.J.; Zhang, J.Y.; Zhang, H.S. Two mono- and dinuclear Ni(II) complexes constructed from quinazoline-type ligands: Synthesis, x-ray structures, spectroscopic, electrochemical, thermal, and antimicrobial studies. *Polyhedron* **2017**, *130*, 100–107. [CrossRef]
26. Chai, L.Q.; Huang, J.J.; Zhang, J.Y.; Li, Y.X. Two 1-D and 2-D cobalt(II) complexes: Synthesis, crystal structures, spectroscopic and electrochemical properties. *J. Coord. Chem.* **2015**, *68*, 1224–1237. [CrossRef]
27. Wang, F.; Gao, L.; Zhao, Q.; Zhang, Y.; Dong, W.K.; Ding, Y.J. A highly selective fluorescent chemosensor for CN^- based on a novel bis(salamo)-type tetraoxime ligand. *Spectrochim. Acta Part A* **2018**, *190*, 111–115. [CrossRef] [PubMed]
28. Dong, Y.J.; Li, X.L.; Zhang, Y.; Dong, W.K. A highly selective visual and fluorescent sensor for Pb^{2+} and Zn^{2+} and crystal structure of Cu^{2+} complex based-on a novel single-armed Salamo-type bisoxime. *Supramol. Chem.* **2017**, *29*, 518–527. [CrossRef]
29. Dong, W.K.; Li, X.L.; Wang, L.; Zhang, Y.; Ding, Y.J. A new application of Salamo-type bisoximes: As a relay-sensor for Zn^{2+}/Cu^{2+} and its novel complexes for successive sensing of H^+/OH^-. *Sens. Actuators B* **2016**, *229*, 370–378. [CrossRef]
30. Wang, B.J.; Dong, W.K.; Zhang, Y.; Akogun, S.F. A novel relay-sensor for highly sensitive and selective detection of Zn^{2+}/Pic^- and fluorescence on/off switch response of H^+/OH^-. *Sens. Actuators B* **2017**, *247*, 254–264. [CrossRef]
31. Dong, W.K.; Akogun, S.F.; Zhang, Y.; Sun, Y.X.; Dong, X.Y. A reversible "turn-on" fluorescent sensor for selective detection of Zn^{2+}. *Sens. Actuators B* **2017**, *238*, 723–734. [CrossRef]
32. Song, X.Q.; Liu, P.P.; Xiao, Z.R.; Li, X.; Liu, Y.A. Four polynuclear complexes based on a versatile salicylamide salen-like ligand: Synthesis, structural variations and magnetic properties. *Inorg. Chim. Acta* **2015**, *438*, 232–244. [CrossRef]
33. Liu, P.P.; Sheng, L.; Song, X.Q.; Xu, W.Y.; Liu, Y.A. Synthesis, structure and magnetic properties of a new one dimensional manganese coordination polymer constructed by a new asymmetrical ligand. *Inorg. Chim. Acta* **2015**, *434*, 252–257. [CrossRef]
34. Song, X.Q.; Liu, P.P.; Liu, Y.A.; Zhou, J.J.; Wang, X.L. Two dodecanuclear heterometallic $[Zn_6Ln_6]$ clusters constructed by a multidentate salicylamide salen-like ligand: Synthesis, structure, luminescence and magnetic properties. *Dalton Trans.* **2016**, *45*, 8154–8163. [CrossRef] [PubMed]

35. Zheng, S.S.; Dong, W.K.; Zhang, Y.; Chen, L.; Ding, Y.J. Four Salamo-type 3d–4f hetero-bimetallic [$Zn^{II}Ln^{III}$] complexes: Syntheses, crystal structures, and luminescent and magnetic properties. *New J. Chem.* **2017**, *41*, 4966–4973. [CrossRef]
36. Liu, Y.A.; Wang, C.Y.; Zhang, M.; Song, X.Q. Structures and magnetic properties of cyclic heterometallic tetranuclear clusters. *Polyhedron* **2017**, *127*, 278–286. [CrossRef]
37. Liu, P.P.; Wang, C.Y.; Zhang, M.; Song, X.Q. Pentanuclear sandwich-type Zn^{II}-Ln^{III} clusters based on a new Salen-like salicylamide ligand: Structure, near-infrared emission and magnetic properties. *Polyhedron* **2017**, *129*, 133–140. [CrossRef]
38. Dong, W.K.; Zheng, S.S.; Zhang, J.T.; Zhang, Y.; Sun, Y.X. Luminescent properties of heterotrinuclear 3d–4f complexes constructed from a naphthalenediol-based acyclic bis(salamo)-type ligand. *Spectrochim. Acta Part A* **2017**, *184*, 141–150. [CrossRef] [PubMed]
39. Wang, L.; Li, X.Y.; Zhao, Q.; Li, L.H.; Dong, W.K. Fluorescence properties of heterotrinuclear Zn(II)–M(II) (M = Ca, Sr and Ba) bis(salamo)-type complexes. *RSC Adv.* **2017**, *7*, 48730–48737. [CrossRef]
40. Yang, Y.H.; Hao, J.; Dong, Y.J.; Wang, G.; Dong, W.K. Two znic(II) complexes constructed from a bis(salamo)-type tetraoxime ligand: Syntheses, crystal structures and luminescence properties. *Chin. J. Inorg. Chem.* **2017**, *33*, 1280–1292.
41. Dong, X.Y.; Li, X.Y.; Liu, L.Z.; Zhang, H.; Ding, Y.J.; Dong, W.K. Tri- and hexanuclear heterometallic Ni(II)–M(II) (M = Ca, Sr and Ba) bis(salamo)-type complexes: Synthesis, structure and fluorescence properties. *RSC Adv.* **2017**, *7*, 48394–48403. [CrossRef]
42. Song, X.Q.; Peng, Y.J.; Chen, G.Q.; Wang, X.R.; Liu, P.P.; Xu, W.Y. Substituted group-directed assembly of Zn(II) coordination complexes based on two new structural related pyrazolone based Salen ligands: Syntheses, structures and fluorescence properties. *Inorg. Chim. Acta* **2015**, *427*, 13–21. [CrossRef]
43. Dong, W.K.; Zhang, F.; Li, N.; Xu, L.; Zhang, Y.; Zhang, J.; Zhu, L.C. Trinuclear cobalt(II) and zinc(II) salamo–type complexes: Syntheses, crystal structures, and fluorescent properties. *Z. Anorg. Allg. Chem.* **2016**, *642*, 532–538. [CrossRef]
44. Song, X.Q.; Cheng, G.Q.; Liu, Y.A. Enhanced Tb(III) luminescence by d^{10} transition metal coordination. *Inorg. Chim. Acta* **2016**, *450*, 386–394. [CrossRef]
45. Wang, L.; Hao, J.; Zhai, L.X.; Zhang, Y.; Dong, W.K. Synthesis, crystal structure, luminescence, electrochemical and antimicrobial properties of bis(salamo)-based Co(II) complex. *Crystals* **2017**, *7*, 277. [CrossRef]
46. Lu, W.G.; Su, C.Y.; Lu, T.B.; Jiang, L.; Chen, J.M. Two stable 3D metal-organic frameworks constructed by nanoscale cages via sharing the single-layer walls. *J. Am. Chem. Soc.* **2006**, *128*, 34–35. [CrossRef] [PubMed]
47. Zhou, H.C.; Kitagawa, S. Metal-organic frameworks (MOFs). *Chem. Soc. Rev.* **2014**, *43*, 5415–5418. [CrossRef] [PubMed]
48. Hao, J.; Li, L.L.; Zhang, J.T.; Akogun, S.F.; Wang, L.; Dong, W.K. Four homo- and hetero-bismetallic 3d/3d-2s complexes constructed from a naphthalenediol-based acyclic bis(salamo)-type tetraoxime ligand. *Polyhedron* **2017**, *134*, 1–10. [CrossRef]
49. Xu, L.; Zhu, L.C.; Ma, J.C.; Zhang, Y.; Zhang, J.; Dong, W.K. Syntheses, structures and spectral properties of mononuclear Cu^{II} and dimeric Zn^{II} complexes based on an asymmetric Salamo-type N_2O_2 ligand. *Z. Anorg. Allg. Chem.* **2015**, *641*, 2520–2524. [CrossRef]
50. Dong, X.Y.; Gao, L.; Wang, F.; Zhang, Y.; Dong, W.K. Tri- and mono-nuclear zinc(II) complexes based on half- and mono-salamo chelating ligands. *Crystals* **2017**, *7*, 267. [CrossRef]
51. Dong, Y.J.; Ma, J.C.; Zhu, L.C.; Dong, W.K.; Zhang, Y. Four 3d–4f heteromultinuclear zinc(II)–lanthanide(III) complexes constructed from a distinct hexadentate N_2O_2-type ligand: Syntheses, structures and photophysical properties. *J. Coord. Chem.* **2017**, *70*, 103–115. [CrossRef]
52. Dong, W.K.; Ma, J.C.; Zhu, L.C.; Zhang, Y. Nine self–assembled nickel(II)-lanthanide(III) heterometallic complexes constructed from a Salamo–type bisoxime and bearing N- or O-donor auxiliary ligand: Syntheses, structures and magnetic properties. *New J. Chem.* **2016**, *40*, 6998–7010. [CrossRef]
53. Dong, W.K.; Ma, J.C.; Zhu, L.C.; Zhang, Y. Self-assembled zinc(II)-lanthanide(III) heteromultinuclear complexes constructed from 3-MeOsalamo ligand: Syntheses, structures and luminescent properties. *Cryst. Growth Des.* **2016**, *16*, 6903–6914. [CrossRef]
54. Akine, S.; Taniguchi, T.; Dong, W.K.; Masubuchi, S.; Nabeshima, T. Oxime-based salen-type tetradentate ligands with high stability against imine metathesis reaction. *J. Org. Chem.* **2005**, *70*, 1704–1711. [CrossRef] [PubMed]

55. Sheldrick, G.M. *SHELXS-2016, Program for Crystal Structure Solution*; University of Göttingen: Göttingen, Germany, 2016.
56. Sheldrick, G.M. *SHELXL-2016, Program for Crystal Structure Refinement*; University of Göttingen: Göttingen, Germany, 2016.
57. Wang, P.; Zhao, L. Synthesis and crystal structure of supramolecular copper(II) complex based on N_2O_2 coordination sphere. *Asian J. Chem.* **2015**, *4*, 1424–1426. [CrossRef]
58. Chai, L.Q.; Wang, G.; Sun, Y.X.; Dong, W.K.; Zhao, L.; Gao, X.H. Synthesis, crystal structure, and fluorescence of an unexpected dialkoxo-bridged dinuclear copper(II) complex with bis(salen)-type tetraoxime. *J. Coord. Chem.* **2012**, *65*, 1621–1631. [CrossRef]
59. Wang, L.; Kang, Q.P.; Hao, J.; Zhang, Y.; Bai, Y.; Dong, W.K. Two trinuclear cobalt(II) salamo–type complexes: Syntheses, crystal structures, solvent effect and fluorescent properties. *Chin. J. Inorg. Chem.* **2018**, *34*, 525–533.
60. Wang, L.; Ma, J.C.; Dong, W.K.; Zhu, L.C.; Zhang, Y. A novel Self–assembled nickel(II)–cerium(III) heterotetranuclear dimer constructed from N_2O_2-type bisoxime and terephthalic acid: Synthesis, structure and photophysical properties. *Z. Anorg. Allg. Chem.* **2016**, *642*, 834–839. [CrossRef]
61. Peng, Y.D.; Li, X.Y.; Kang, Q.P.; An, G.X.; Zhang, Y.; Dong, W.K. Synthesis and fluorescence properties of asymmetrical salamo-type tetranuclear zinc(II) complex. *Crystals* **2018**, *8*, 107. [CrossRef]
62. Gao, L.; Wang, F.; Zhao, Q.; Zhang, Y.; Dong, W.K. Mononuclear Zn(II) and trinuclear Ni(II) complexes derived from a coumarin-containing N_2O_2 ligand: Syntheses, crystal structures and fluorescence properties. *Polyhedron* **2018**, *139*, 7–16. [CrossRef]
63. Dong, X.Y.; Kang, Q.P.; Jin, B.X.; Dong, W.K. A dinuclear nickel(II) complex derived from an asymmetric Salamo-type N_2O_2 chelate ligand: Synthesis, structure and optical properties. *Z. Naturforsch.* **2017**, *72*, 415–420. [CrossRef]
64. Gao, L.; Liu, C.; Wang, F.; Dong, W.K. Tetra-, penta- and hexa-coordinated transition metal complexes constructed from coumarin-containing N_2O_2 ligand. *Crystals* **2018**, *8*, 77. [CrossRef]
65. Addison, A.W.; Rao, T.N.; Reedijk, J.; Rijn, J.V.; Verschoor, G.C. Synthesis, structure, and spectroscopic properties of copper(II) compounds containing nitrogen–sulphur donor ligands; the crystal and molecular structure of aqua[1,7-bis(*N*-methylbenzimidazol-2′-yl)-2,6-dithiaheptane]copper(II) perchlorate. *J. Chem. Soc. Dalton Trans.* **1984**, *7*, 1349–1356. [CrossRef]
66. Zhao, L.; Dang, X.T.; Chen, Q.; Zhao, J.X.; Wang, L. Synthesis, Crystal structure and spectral properties of a 2D supramolecular copper(II) complex with 1-(4-{[(*E*)-3-ethoxyl-2-hydroxybenzylidene]amino}phenyl)ethanone oxime. *Synth. React. Inorg. Met.-Org. Nano-Met. Chem.* **2013**, *43*, 1241–1246. [CrossRef]
67. Li, G.; Hao, J.; Liu, L.Z.; Zhou, W.M.; Dong, W.K. Syntheses, crystal structures and thermal behaviors of two supramolecular salamo-type cobalt(II) and zinc(II) complexes. *Crystals* **2017**, *7*, 217. [CrossRef]
68. Chen, L.; Dong, W.K.; Zhang, H.; Zhang, Y.; Sun, Y.X. Structural variation and luminescence properties of tri- and dinuclear Cu^{II} and Zn^{II} complexes constructed from a naphthalenediol-based bis(Salamo)-type ligand. *Cryst. Growth Des.* **2017**, *17*, 3636–3648. [CrossRef]
69. Ma, J.C.; Dong, X.Y.; Dong, W.K.; Zhang, Y.; Zhu, L.C.; Zhang, J.T. An unexpected dinuclear Cu(II) complex with a bis(Salamo) chelating ligand: Synthesis, crystal structure, and photophysical properties. *J. Coord. Chem.* **2016**, *69*, 149–159. [CrossRef]
70. Tao, C.H.; Ma, J.C.; Zhu, L.C.; Zhang, Y.; Dong, W.K. Heterobimetallic 3d–4f Zn(II)–Ln(III) (Ln=Sm, Eu, Tb and Dy) complexes with a N_2O_4 bisoxime chelate ligand and a simple auxiliary ligand Py: Syntheses, structures and luminescence properties. *Polyhedron* **2017**, *128*, 38–45. [CrossRef]
71. Yang, X.P.; Ben, J.M.; Hahn, P.; Jones, R.A.; Wong, W.K.; Stevenson, K.J. Synthesis of an octanuclear Eu(III) cage from Eu_4^{2+}: Chloride anion encapsulation, luminescence, and reversible MeOH adsorption via a porous supramolecular architecture. *Inorg. Chem.* **2007**, *46*, 7050–7054. [CrossRef] [PubMed]
72. Dong, Y.J.; Dong, X.Y.; Dong, W.K.; Zhang, Y.; Zhang, L.S. Three asymmetric Salamo-type copper(II) and cobalt(II) complexes: Syntheses, structures, fluorescent properties. *Polyhedron* **2017**, *123*, 305–315. [CrossRef]